Accepted Manuscript

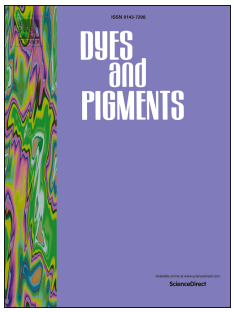

Influence of integrated alkyl-chain length on the mesogenic and photophysical properties of platinum-based metallomesogens and their application for polarized white OLEDs

Yafei Wang, Jiang Fan, Junwei Shi, Hongrui Qi, Etienne Baranoff, Guohua Xie, Qingguo Li, Hua Tan, Yu Liu, Weiguo Zhu

PII: S0143-7208(16)30214-5

DOI: 10.1016/j.dyepig.2016.05.024

Reference: DYPI 5256

To appear in: *Dyes and Pigments*

Received Date: 2 April 2016

Revised Date: 11 May 2016

Accepted Date: 14 May 2016

Please cite this article as: Wang Y, Fan J, Shi J, Qi H, Baranoff E, Xie G, Li Q, Tan H, Liu Y, Zhu W, Influence of integrated alkyl-chain length on the mesogenic and photophysical properties of platinum-based metallomesogens and their application for polarized white OLEDs, *Dyes and Pigments* (2016), doi: 10.1016/j.dyepig.2016.05.024.

Graphical Abstract

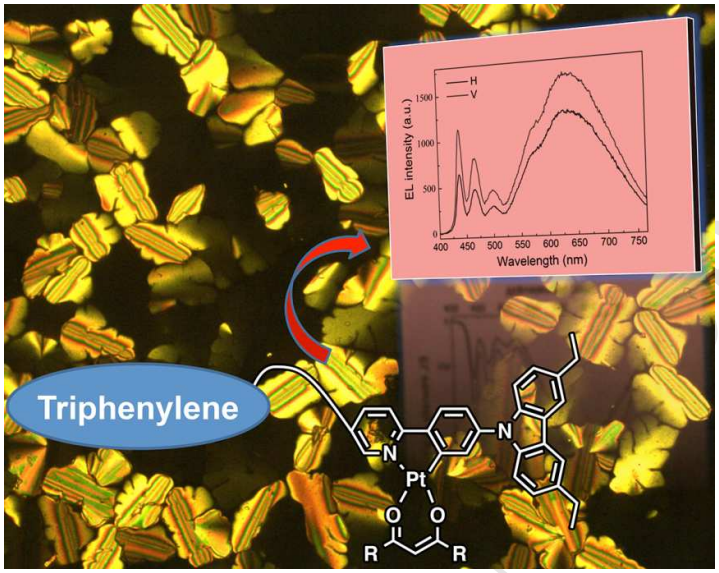

Influence of Integrated Alkyl-Chain Length on the Mesogenic and Photophysical Properties of Platinum-Based Metallomesogens and Their Application for Polarized White OLEDs

Yafei Wang†‖*, Jiang Fan†, Junwei Shi†, Hongrui Qi†, Etienne Baranoff^Δ, Guohua Xie‡*, Qingguo Li&, Hua Tan†, Yu Liu†, Weiguo Zhu†*

†*College of Chemistry, Key Lab of Environment-Friendly Chemistry and Application of the Ministry of Education, Xiangtan University, Xiangtan 411105, China*

‡*Hubei Collaborative Innovation Center for Advanced Organic Chemical Materials, Hubei Key Lab on Organic and Polymeric Optoelectronic Materials, Department of Chemistry, Wuhan University, Wuhan 430072, China.*

Δ *School of Chemistry, University of Birmingham, Edgbaston, Birmingham, B15 2TT, UK*

&college of Chinese medicines, Guangzhou University of Chinese medicine, Guangzhou 510640, China

‖*Institute of Polymer Optoelectronic Materials and Devices, State Key Laboratory of Luminescent Materials and Devices, South China University of Technology, Guangzhou 510640, China*

*To whom correspondence should be addressed

(G. Xie) xgh-008@163.com

(W. Zhu) zhuwg18@126.com

(Y. Wang) qiji830404@hotmail.com

Abstract

In this context, a series of platinum complexes containing a triphenylene unit, namely **Pt5-Pt8**, was prepared and characterized. Platinum complex **Pt6** shows a clearly column liquid crystalline property, confirmed by differential scanning calorimetry, polarized optical microscopy and X-ray diffraction. These platinum complexes only display monomolecular emission both in solution and in neat film, an effect attributed to the presence of carbazole as a bulky group disfavoring aggregation of the complexes. Hole mobilities in the range of 10^{-5}–10^{-6} cm^2 V^{-1} s^{-1} were obtained for the annealed platinum complexes films. It was found that the method to align the emissive layer has a crucial role on the performance of the devices. The first example of polarized phosphorescent white OLED with polarized ratio of 1.4 was achieved in **Pt6**-based device. This research opens up a new aspect of phosphorescent metallomesogens application for polarized white light emission.

Keywords: Platinum metallomesogens; Liquid crystalline; Luminescence; Polarized OLEDs

1. Introduction

Over the last two decades, square planar d^8 platinum complexes have attracted intensive attention as phosphors in organic light-emitting diodes (OLEDs) due to their high spin-orbit coupling constants and diverse excited states, such as metal-to-ligand charge transfer (MLCT), metal-metal-to-ligand charge transfer (MMLCT), ligand center charge transfer (LC), interligand charge transfer (ILCT) [1-4]. To date, OLEDs using platinum complexes with high efficiency across the whole visible and near-infrared region have been realized [5-8]. Yet, these devices generally emit light without polarization, which makes them unsuitable for applications such as the backlight of liquid crystal displays (LCDs) and three-dimension (3D) imaging systems [9-12].

Polarized emission is usually obtained with a polarizer and a non-polarized light source. Consequently, more than 50% of the produced light is wasted due to absorption by the polarizer. To solve this issue and improve the energy efficiency of polarized light sources, imparting liquid crystalline properties to luminescent materials has been intensively studied as a strategy to directly obtain polarized emission [13]. Since the first example of linearly polarized electroluminescence (EL) was reported by Dyreklev *et al.* using an aligned polymer film [14], the research focusing on polarized emission from fluorescent liquid crystal molecules and polymers has flourished [15-22]. However, fluorescent materials can harvest only singlet excitons, which further limits the efficiency of electroluminescent devices.

Phosphorescent square planar platinum complexes appear very promising in view

of achieving efficient polarized electroluminescence: by harvesting both singlet and triplet excitons they could lead to 100% internal quantum efficiency and their planar structure favor the formation of liquid crystalline phases and promotes charge mobility in OLEDs. Efforts have been particularly devoted to developing arylpyridine derivative based platinum metallomesogens [23-36]. Although these platinum metallomesogens showed intense emission both in solution and in solid state [37-41], the investigation of the polarized emission is still limited, with only few reported examples. The first study of the polarized EL emission using mesogenic platinum complex was reported by Liu *et al.*, in which a *R* (polarized ratio) of 2, maximum luminance of 2000 cd/m^2 and current efficiency of 2.4 cd/A were observed [38].

In our previous work, mononuclear and dinuclear platinum-based metallomesogens bearing 2-phenylpyridine ligand showed a polarized ratio up to 10.7 in PL emission after annealing the complexes on a pre-aligned polyimide film [40,41]. Considering the stacking of discotic mesogens into extended one-dimensional column liquid crystals [42], most recently, we successfully combined discotic mesogens such as triphenylenes with platinum complex and thus obtained new metallomesogens with columnar phases [43,44]. Encouraged by these results, a new series of platinum bearing triphenylene and carbazole units, namely **Pt5-Pt8**, were designed and prepared (**Chart 1**). In order to explore the structure-property relationship, the alkyl-chains between triphenylene moiety and platinum skeleton varied from conjugation to non-conjugation. To enhance the emission efficiency and the thermal stability, carbazole unit was grafted onto the cyclometalated ligand. All these platinum

complexes were characterized by ^{1}H NMR, ^{13}C NMR, MALDI TOF-MS and elemental analysis. The mesomorphic behavior was studied by differential scanning calorimetry (DSC), polarized optical microscopy (POM) and X-ray diffraction (XRD), while the optophysical properties were investigated with UV-visible absorption, PL emission, cyclic voltammetry (CV) and hole mobility measurements. Polarized OLEDs were fabricated using **Pt5** and **Pt6** as the dopants, respectively, and the first example of polarized white emission using platinum complex was obtained for **Pt6** doped device.

2. Experimental section

2.1. Materials and measurement

All reagents were purchased from *J&K* Chemical and Aladdin companies. All reactions were carried out under N_2 atmosphere. Compounds **6** and monohydroxypentaalkoxytriphenylene (**10**) were reported in previous literatures [42,45]. ^{1}H NMR and ^{13}C NMR spectra were acquired using a Bruker Dex-400 NMR instrument using $CDCl_3$ as a solvent. Mass spectra (MS) were recorded on a Bruker Autoflex MALDI-TOF instrument using dithranol as a matrix. Elemental analysis was determined by Vario EL III. The UV-vis absorption and PL spectra were measured with a Varian Cray 50 and Perkin-Elmer LS50B luminescence spectrometer, respectively. Solutions of ppyPtacac (Φ_{PL} = 0.15) in 2-methyltetrahydrofuran were used as a reference [4]. The equation $\Phi_s = \Phi_r(\eta_s^2 A_r I_s / \eta_r^2 A_s I_r)$ was used to calculate the quantum yields. Thermogravimetric analysis (TGA) was carried out with a

NETZSCH STA449 from 25 to 600 ℃ at a 20 ℃/min heating rate under N_2 atmosphere. Differential scanning calorimerty (DSC) was measured at the phase transition temperature with a rate of 10 ℃/min on the first cooling and second heating process. Polarized optical microscopy (POM) was recorded the birefringent phenomenon with a rate of 1 ^{o}C/min on cooling process. X-ray diffraction was measured by Bruker D8 Discover diffractometer with a 2D Vantec detector. The sample was mounted in a capillary in a bespoke heating environment-a hollow graphite furnace-with temperature control via an Eurotherm controller.

2.2. Devices fabrication and characterization

A layer of poly(3,4-ethylenedioxythiophene): poly(styrenesulfonate) (PEDOT:PSS) was spin-coated on the ITO glass substrate after UV-ozone treatment. After baking of PEDOT:PSS at 120 ℃ for 10 mins, another layer of poly(*N*-vinylcarbazole) (PVK) was spin-coated directly and then baked at 120 ℃ for another 10 mins. In order to obtain polarized emission, we managed to pattern the emitting layer via different methods (annealing or rubbing, see below) after spin-coating of the platinum complex doped poly(9,9-dioctylfluorene) (PFO) onto the hole transporting layer PVK. An electron transporting layer of bis-4,6-(3,5-di-3-pyridylphenyl)-2-methylpyrimidine (B3PYMPM) was thermally evaporated on the emitting layer after deliberate treatments. To compare the influence of the treatment of the emitting layer on the polarized emission, we constructed several devices with different treatments of the emitting layer. The device configurations are listed as below:

Devices I: ITO/PEDOT:PSS (30 nm)/PVK (30 nm)/PFO:Pt6 (80:20, 70 nm, no

baking)/B3PYMPM(50 nm)/Ca (100 nm)/Al (100 nm).

Devices II: ITO/PEDOT:PSS (30 nm)/PVK (30 nm)/PFO:Pt6 (80:20, 70 nm, baked at 120°C for 10 min)/B3PYMPM (50 nm)/Ca (100 nm)/Al (100 nm).

Devices III: ITO/PEDOT:PSS (30 nm)/PVK (30 nm)/PFO:Pt6 (80:20, 70 nm, rubbed and then baked at 120°C for 10 min)/B3YMPM (50 nm)/Ca (100 nm)/Al (100 nm).

Devices IV: ITO/PEDOT:PSS (30 nm)/PVK (30 nm)/PFO:Pt6 (80:20, 70 nm, pressed and then baked at 120°C for 10 min)/B3YMPM (50 nm)/Ca (100 nm)/Al (100 nm).

All the devices were encapsulated under a nitrogen atmosphere using UV curable epoxy. The current-voltage-luminance characteristics were collected with a PR735 spectrascan spectrometer and a Keithley 2400 programmable source meter. The (polarized) EL spectra were recorded by an Ocean Optics USB2000 spectrometer. The EL intensities parallel and perpendicular to the rubbing direction (along the ITO stripe) could be distinguished by aligning a linear polarizer inserted between the OLEDs and the spectrometer at two mutually perpendicular directions which were denoted as H (horizon) and V (vertical).

2.3. Hole mobilities

The hole mobility was measured using the space charge limited current (SCLC) model with a devices configuration of ITO/PEDOT:PSS (40 nm)/Active Layer (100 nm)/MoO_3 (10 nm)/Ag (100 nm). The active layer is annealed for 30 mins. The PEDOT:PSS was spin-coated onto the ITO glass at 4000 rpm and then baked at 160 ^{o}C for 15 mins in air. The active layer was spin-cast from chloroform (20 mg/mL) at 1000 rpm. A MoO_3 and Ag cathode was then thermally evaporated under vacuum (~

10^{-7} torr) through a shadow mask defining an active device area of ~0.03 cm^2. The SCLC is described by: $J = (9/8)\varepsilon_0\varepsilon_r\mu(V^2/d^3)$, where J is the current density, d is the film thickness of the active layer, μ_0 is the hole mobility, ε_r is the relative dielectric constant of the transport medium, ε_0 is the permittivity of free space (8.85×10^{-12} F m^{-1}), V is the internal voltage in the device.

2.4. Synthesis

3,6-diacetyl-9*H*-carbazole (1)

9H-carbazole (3.0 g, 17.96 mmol) was added to the solution of aluminum chloride (6.8 g, 51.1 mmol) in CH_2Cl_2 (100 mL) and the mixture was cooled to 0 ^oC. Acetyl chloride (3.8 g, 48.7 mmol) was then added dropwise into the mixture at 0 ^oC. After 12 h, the solvent was removed by rotary evaporation. The residue was purified by recrystallization with ethanol to obtain gray solid **1** (2.24 g, 50%). ^1H NMR ($CDCl_3$, 400 MHz, TMS), δ (ppm): 8.78 (s, 2H), 8.68 (s, 1H), 8.15 (d, J = 8.2 Hz, 2H), 7.50 (d, J = 8.48 Hz, 2H), 2.7 (s, 6H).

3,6-diethyl-9*H*-carbazole (2)

A mixture of compound **1** (2.8 g, 11.1 mmol), aluminum chloride (5.93 g, 44.4 mmol) and tetrahydrofuran (THF) (40 mL) was cooled to 0 ^oC. $LiAlH_4$ (1.0 g, 33.3 mmol) was added in small batches. The reaction mixture was stirred for 4 h at room temperature (RT). The solvent was removed by rotary evaporation, and the residue was purified by silica gel column chromatography using petroleum ether (PE)/CH_2Cl_2 (*V:V,* 8/1) as eluent to give **2** as a yellow solid (1.0 g, 40%). ^1H NMR ($CDCl_3$, 400 MHz, TMS), δ (ppm): 7.88 (s, 2H), 7.32 (d, J = 8.21 Hz, 2H), 7.24 (d, J = 8.77 Hz,

2H), 2.85-2.79 (t, *J* = 7.52 Hz, 4H), 1.36-1.11 (m, 6H).

9-(4-bromophenyl)-3,6-diethyl-9*H*-carbazole (3)

A mixture of compound **2** (1.4 g, 6.27 mmol), 1-bromo-4-iodobenzene (2.6 g, 9.4 mmol), potassium carbonate (2.5 g, 18.81 mmol), 1,10-phenanthroline monohydrate (372 mg, 1.88 mmol) in *o*-xylene (100 mL) was refluxed for 24 h under nitrogen atmosphere. After cooling to RT, the reaction mixture was poured into water and extracted with CH_2Cl_2. The organic layer was collected and dried with $MgSO_4$. The solvent was removed by rotary evaporation, and the residue was purified by silica gel column chromatography using PE as eluent to give as faint yellow solid **3** (1.68 g, 71%). ^{1}H NMR (*d*-DMSO, 400 MHz, TMS), δ (ppm): 8.04 (s, 2H), 7.99 (d, *J* = 8.2 Hz, 2H), 7.84 (d, *J* = 8.4 Hz, 2H), 7.58 (d, *J* = 8.4 Hz, 2H), 7.43 (d, *J* = 8.2 Hz, 2H), 2.78 (d, *J* = 7.4 Hz, 4H), 1.30-1.26 (m, 6H).

3,6-diethyl-9-(4-(4,4,5,5-tetramethyl-1,3,2-dioxaborolan)phenyl)-9*H*-carbazole (4)

n-BuLi (1.6 M in hexane, 5.4 mL, 8.64 mmol) was added dropwise into a solution of **3** (1.09 g, 2.88 mmol) in THF (30 mL) at –78 ^{o}C under nitrogen atmosphere. The mixture was stirred at –78 ^{o}C for 2 h, then the solution was stirred for 30 mins at RT. 2-Isopropoxy-4,4,5,5-tetramethyl-1,3,2-dioxaborolane (1.07 g, 5.76 mmol) was added at –78 ^{o}C. The mixture was then allowed to room temperature and stirred overnight. The reaction was quenched by water and the mixture was extracted with CH_2Cl_2. The organic layer was collected and washed with water. After removing the solvent, the residue was purified by silica gel column chromatography using PE as eluent to give

as brown solid **4** (480 mg, 38%). ^{1}H NMR ($CDCl_3$, 400 MHz, TMS), δ (ppm): 8.06 (d, J = 7.9 Hz, 2H), 7.96 (s, 2H), 7.61 (d, J = 7.9 Hz, 2H), 7.40 (d, J = 8.3 Hz, 2H), 7.26 (d, J = 8.4 Hz, 2H), 2.87 (d, J = 7.5 Hz, 4H), 1.53-1.20 (m, 18H).

9-(4-(5-bromopyridin)phenyl)-3,6-diethyl-9*H*-carbazole (5)

A mixture of compound **4** (480 mg, 1.1 mmol), 2,5-dibromopyridine (260 mg, 1.65 mmol), cesium carbonate (1.0 g, 3.3 mmol), tetrakis(triphenylphosphine)palladiun(0) (38 mg, 0.032 mmol) and THF (40 mL) was refluxed for 24 h in nitrogen atmosphere. After cooling to RT, the mixture was extracted with CH_2Cl_2 and washed with water. The solvent was removed by rotary evaporation. The residue was purified by silica gel column chromatography using CH_2Cl_2/PE (*V:V,* 8/1) as eluent to give as faint yellow solid **5** (160 mg, 32%). ^{1}H NMR ($CDCl_3$, 400 MHz, TMS), δ (ppm): 8.82 (s, 1H), 8.21 (d, J = 8.68 Hz, 2H), 7.96 (d, J = 8.78 Hz, 2H), 7.76-7.70 (m, 4H), 7.42 (d, J = 8.2 Hz, 2H), 7.08 (d, J = 7.48 Hz, 1H), 6.94 (d, J = 8.4 Hz, 1H), 2.90-2.85 (m, 4H), 0.90 (m, 6H).

6-(4-(3,6-diethyl-9*H*-carbazol-9-yl)phenyl)nicotinaldehyde (7)

A mixture of compound **4** (500 mg, 1.2 mmol), 2-bromine-5-pyridinecarboxaldehyde (271 mg, 1.46 mmol), tetrakis(triphenylphosphine)palladium(0) (42 mg, 0.036 mmol), cesium carbonate (4.14 g, 3.63 mmol) and toluene/ethanol (15 mL/15 mL) was heated to 80 ^{o}C for 24 h in nitrogen atmosphere. After cooling to RT, the mixture was extracted with CH_2Cl_2 (3 × 20 mL). The organic layer was collected and washed with water. The solvent was removed by rotary evaporator, and the residue was purified by silica gel column chromatography using PE/ethyl acetate (EA) (*V:V,* 10/1) as eluent to

give as a faint yellow solid **7** (270 mg, 55%). ^{1}H NMR ($CDCl_3$, 400 MHz, TMS), δ (ppm): 8.72 (s, 1H), 8.20 (d, J = 8.63 Hz, 2H), 7.92 (d, J = 8.76 Hz, 2H), 7.72-7.69 (m, 4H), 7.40 (d, J = 8.21 Hz, 2H), 7.06 (d, J = 7.42 Hz, 1H), 6.92 (d, J = 8.30 Hz, 1H), 2.88-2.83 (m, 4H), 1.30 (m, 6H).

(6-(4-(3,6-diethyl-9*H*-carbazol-9-yl)phenyl)pyridin-3-yl)methanol (8)

Compound **7** (270 mg, 0.66 mmol) and $NaBH_4$ (112 mg, 1.66 mmol) in toluene/ethanol (15 mL/15 mL) was stirred for 6 h at RT. Water was added to quench the reaction, and the mixture was extracted with ethyl acetate (3 × 20 mL). The organic layer was collected, washed with water and then dried with anhydrous $MgSO_4$. After removed the solvent, the residue was purified by silica gel column chromatography using EA as eluent to give as yellow solid **8** (210 mg, 78%). ^{1}H NMR ($CDCl_3$, 400 MHz, TMS), δ (ppm): 8.72 (s, 1H), 8.20 (d, J = 8.28 Hz, 2H), 7.94 (s, 2H), 7.85 (d, J = 8.04 Hz, 1H), 7.82 (d, J = 8.08 Hz, 1H), 7.67 (d, J = 8.28 Hz, 2H), 7.40 (d, J = 8.32 Hz, 2H), 7.24 (d, J = 8.04 Hz, 2H), 4.84 (s, 2H), 2.87-2.81 (m, 4H), 1.35 (t, J = 7.52 Hz, 6H).

9-(4-(5-((6-bromohexyloxy)methyl)pyridin-2-yl)phenyl)-3,6-diethyl-9*H*-carbazole (9)

A mixture of compound **8** (250 mg, 0.61 mmol), 1,6-dibromohexane (179 mg, 0.74 mmol), potassium iodide (3.05 mg, 0.018 mmol), saturated sodium hydroxide (73 mg) and actone (20 mL) was refluxed 24 h in nitrogen atmosphere. After cooling to RT, the mixture was extracted with CH_2Cl_2 (3 × 20 mL). The organic layer was collected, washed with water and dried with anhydrous $MgSO_4$. The solvent was removed by

rotary evaporation, and then the residue was purified by silica gel column chromatography using PE/EA (*V:V,* 10/1) as eluent to give as yellow solid **9** (70 mg, 20%). ^{1}H NMR ($CDCl_3$, 400 MHz, TMS), δ (ppm): 8.68 (s, 1H), 8.19 (d, *J* = 7.16 Hz, 2H), 7.94 (s, 2H), 7.81 (s, 2H), 7.67 (d, *J* = 7.08 Hz, 2H), 7.40 (d, *J* = 7.72 Hz, 2H), 7.25 (s, 2H), 4.58 (s, 2H), 3.54 (s, 2H), 3.42 (s, 2H), 3.19 (s, 2H), 2.84 (t, *J* = 6.88 Hz, 4H), 1.89-1.43 (m, 6H), 1.34 (t, *J* = 6.4 Hz, 6H).

Compound LG-1

A mixture of compound **5** (220 mg, 0.48 mmol), compound **6** (220 mg, 0.48 mmol), tetrakis (triphenylphosphine)palladiun(0) (17 mg, 0.014 mmol), cesium carbonate (2 mol/L, 6 mL) and toluene 20 mL was heated to 80 ^{o}C for 24 h in nitrogen atmosphere. After cooling to RT, the reaction was quenched by water and the mixture was extracted with CH_2Cl_2. The organic layer was collected, washed with water and dried with anhydrous $MgSO_4$. The solvent was removed by rotary evaporation and the residue was purified by silica gel column chromatography using PE/CH_2Cl_2 (*V:V*, 10/8) as the eluent to give as yellow solid **LG-1** (290 mg, yield 54%). ^{1}H NMR ($CDCl_3$, 400 MHz, TMS), δ (ppm): 9.20 (s, 1H), 8.72 (s, 1H), 8.61 (d, *J* = 8.6 Hz, 1H), 8.31 (d, *J* = 8.34 Hz, 2H), 8.21 (d, *J* = 6.18 Hz, 3H), 7.98 (t, *J* = 7.9 Hz, 3H), 7.87 (d, *J* = 5.44 Hz, 3H), 7.72 (d, *J* = 8.34 Hz, 2H), 7.44 (d, *J* = 8.32 Hz, 2H), 7.28 (m, 2H), 4.28 (t, *J* = 7.48 Hz, 8H), 2.88-2.83 (m, 4H), 1.96 (t, *J* = 7.16 Hz, 8H), 1.61-1.25 (m, 40H), 0.92 (m, 18H). ^{13}C NMR (100 MHz, $CDCl_3$), δ (ppm): 14.05, 15.51, 16.41, 22.67, 25.98, 26.22, 28.95, 29.13, 29.33, 31.90, 63.92, 66.64, 68.26, 68.55, 69.58, 69.70, 69.84, 107.41, 109.65, 114.09, 118.98, 120.26, 121.28, 123.40, 123.91, 124.72,

126,95, 128.19, 128.80, 129.47, 131.69, 134.85, 135.32, 136.07, 137.56, 139.06, 139.47, 148.47, 149.39, 150.03, 155.25. MALDI-MS (m/z): calcd. for $C_{77}H_{98}N_2O_4$ [M^+] 1114.75, found 1114.87.

Compound LG-2

A mixture of compound **10** (822 mg, 0.93 mmol), compound **9** (353 mg, 0.62 mmol), potassium carbonate (855 mg, 6.2 mmol) and potassium iodide (51 mg, 0.31 mmol) in acetone (20 mL) was refluxed for 24 h in nitrogen atmosphere. After cooled to RT, the mixture was extracted with CH_2Cl_2 (3 × 30 mL). The organic layer was collected, washed with water and dried with anhydrous $MgSO_4$. The solvent was removed by rotary evaporation and was purified by silica gel column chromatography using PE/EA (*V:V,* 10/1) as eluent to give as yellow solid **LG-2** (574 mg, 54%). ^{1}H NMR ($CDCl_3$, 400 MHz, TMS), δ (ppm): 8.67 (s, 1H), 8.14 (d, J = 7.8 Hz, 2H), 7.94 (s, 2H), 7.83-7.77 (m, 6H), 7.71 (d, J = 7.76 Hz, 2H), 7.62 (d, J = 7.76 Hz, 2H), 7.38 (d, J = 8.16 Hz, 2H), 7.25 (s, 2H), 4.58 (s, 2H), 4.22-4.21 (m, 12H), 3.5 (s, 2H), 2.85 (s, 4H), 1.92 (m, 12H), 1.36-1.15 (m, 60H), 0.80(m, 15H). ^{13}C NMR (100 MHz, $CDCl_3$), δ (ppm): 14.15, 14.60, 16.42, 22.81, 26.0, 26.31, 29.41, 29.73, 29.82, 31.90, 32.71, 60.25, 69.38, 69.56, 72.18, 76.20, 106.23, 107.38, 109.52, 111.12, 117.23, 118.90, 121.24, 122.11, 123.70, 126.21, 133.12, 136.47, 138.36, 139.70, 146.52, 147.87, 148.26, 149.90. MALDI-MS (m/z): calcd. for $C_{92}H_{128}N_2O_7$ [M^+] 1374.01, found 1374.34.

Generation procedures for synthesis platinum complexes

Cyclometalated ligand (**LG-1**/**LG-2**) (2.2 eq) and K_2PtCl_4 (1.0 eq) in a mixture of

chloroform (4 mL), distilled water (2 mL) and 2-ethoxyethanol (6 mL) was heated to 80 ^{o}C for 24 h in nitrogen atmosphere. After cooling to RT, the reaction mixture was extracted with CH_2Cl_2, and the organic layer was collected and dried with Na_2SO_4. After removed the solvent, the dimer was obtained and used to the next step without any further purification.

A mixture of dimer (1.0 eq), ancillary ligand (3.0 eq), sodium carbonate (10.0 eq) and 2-ethoxyethanol was heated to 100 ^{o}C for 24 h in nitrogen atmosphere. After cooling to RT, the reaction mixture was poured into water and extracted with CH_2Cl_2. The organic layer was collected and dried with anhydrous Na_2SO_4. The organic solvent was removed by rotary evaporation and the residue was passed through a flash silica gel column to give the platinum complexes.

Pt5: PE/CH_2Cl_2 (*V:V*, 2/1), yellow solid, (40 mg, yield 12.5%). ^{1}H NMR ($CDCl_3$, 400 MHz, TMS), δ (ppm): 9.49 (s, 1H), 8.69 (s, 1H), 8.65 (d, J = 8.4 Hz, 1H), 8.26 (d, J = 8.1 Hz, 1H), 8.25 (s, 1H), 8.11 (s, 1H), 7.97 (s, 1H), 7.87 (t, J = 8.0 Hz, 4H), 7.80 (d, J = 8.2 Hz, 3H), 7.70 (d, J = 8.0 Hz, 1H), 7.54 (d, J = 8.2 Hz, 2H), 7.33 (d, J = 7.8 Hz, 2H), 5.5 (s, 1H). 4.28 (t, J = 7.48 Hz, 8H), 2.88-2.84 (m, 4H), 1.96 (t, J = 7.16 Hz, 8H), 1.61-1.12 (m, 44H), 0.92 (m, 18H). ^{13}C NMR (100 MHz, $CDCl_3$), δ (ppm): 14.14, 16.50, 22.73, 26.25, 26.28, 26.29, 27.13, 28.46, 28.99, 29.38, 29.40, 29.49, 29.54, 29.62, 31.90, 69.40, 69.53, 69.65, 70.00, 102.53, 107.00, 110.31, 118.74, 120.81, 121.68, 123.15, 123.29, 123.58, 123.96, 124.06, 124.50, 124.87, 125.96, 128.88, 129.35, 133.17, 135.59, 136.27, 138.16, 139.56, 143.12, 145.46, 149.19, 149.29, 149.97, 150.15, 165.16, 184.41, 185.56. MALDI-MS (m/z): calcd. for

$C_{82}H_{104}N_2O_6Pt$ [M^+] 1407.75, found 1407.84. Anal. Calcd for $C_{82}H_{104}N_2O_6Pt$: C, 69.91; H, 7.44; N, 1.99. Found: C, 70.07; H, 7.41; N, 1.90.

Pt6: PE/CH_2Cl_2 (*V:V*, 10/7), yellow solid (90 mg, yield 37.6%). ^{1}H NMR ($CDCl_3$, 400 MHz, TMS), δ (ppm): 9.72 (s, 1H), 8.74 (s, 1H), 8.57 (d, *J* = 8.3 Hz, 1H), 8.06 (d, *J* = 8.3 Hz, 1H), 8.05 (s, 1H), 7.88 (s, 1H), 7.78-7.76 (m, *J* = 8.3 Hz, 8H), 7.73-7.72 (d, *J* = 6.4 Hz, 6H), 7.45 (d, *J* = 7.52 Hz, 1H), 7.31 (m, 2H), 6.67 (d, *J* = 8.4 Hz, 2H), 6.2 (d, *J* = 8.2 Hz, 2H), 6.5 (s, 1H), 4.30-4.24 (t, *J* = 6.3 Hz, 8H), 4.30-4.24 (t, *J* = 6.3 Hz, 8H), 3.79 (t, *J* = 6.3 Hz, 4H) 2.91-2.90 (m, 4H), 1.98 (t, *J* = 6.6 Hz, 8H), 1.68-1.27 (m, 78H), 0.93-0.85 (m, 18H). ^{13}C NMR(100 MHz, $CDCl_3$), δ (ppm): 14.05, 14.06, 16.52, 22.66, 22.69, 26.28, 29.29, 29.36, 29.38, 29.43, 29.52, 29.56, 29.60, 29.63, 29.70, 29.75, 31.90, 31.94, 67.84, 69.04, 69.63, 69.80, 69.90, 107.49, 110.80, 113.92, 114.31, 118.71, 123.32, 123.84, 124.01, 124.34, 124.39, 124.66, 126.02, 128.54, 128.66, 128.82, 129.51, 131.81, 133.89, 134.46, 135.75, 139.06, 145.54, 149.37, 149.49, 149.86, 150.12, 161.10, 161.41, 177.11, 177.60. MALDI-MS (m/z): calcd. for $C_{116}H_{156}N_2O_8Pt$ [M^+] 1900.15, found 1900.20. Anal. Calcd for $C_{116}H_{156}N_2O_8Pt$: C, 73.27; H, 8.27; N, 1.47. Found: C, 72.23; H, 8.09; N, 1.48.

Pt7: PE/CH_2Cl_2 (*V:V*, 1/1), yellow solid (300 mg, 57%). ^{1}H NMR ($CDCl_3$, 400 MHz, TMS), δ (ppm):8.67 (s, 1H), 8.14 (d, *J* = 7.8 Hz, 2H), 7.94 (s, 2H), 7.83-7.77 (m, 6H), 7.71 (d, *J* = 7.76 Hz, 2H), 7.62 (d, *J* = 7.76 Hz, 2H), 7.38 (d, *J* = 8.16 Hz, 2H), 7.25 (s, 1H), 5.42 (s, 1H), 4.58 (s, 2H), 4.22-4.21 (m, 12H), 3.5 (s, 2H), 2.85 (s, 4H), 1.92 (m, 12H), 1.36-1.15 (m, 66H), 0.80 (m, 18H). ^{13}C NMR (100 MHz, $CDCl_3$), δ (ppm): 14.15, 16.65, 22.73, 25.89, 25.99, 26.26, 26.39, 29.43, 29.56, 29.62, 29.68, 29.73,

31.90, 31.97, 67.79, 69.25, 69.85, 69.91, 70.67, 107.47, 110.51, 114.14, 118.77, 123.38, 123.84, 124.19, 125.99, 128.76, 128.85, 135.71, 137.42, 139.57, 148.92, 149.03, 149.11, 184.39, 185.74. MALDI-MS (m/z): calcd. for $C_{97}H_{134}N_2O_9Pt$ [M^+] 1665.97, found 1666.3, 1567.22. Anal. Calcd for $C_{97}H_{134}N_2O_9Pt$: C, 69.88; H, 8.10; N, 1.68 Found: C, 67.94; H, 7.94; N, 1.72.

Pt8: PE/CH_2Cl_2 (*V:V*, 1/1), yellow solid, (70 mg, 30.7%). ^{1}H NMR ($CDCl_3$, 400 MHz, TMS), δ (ppm): 9.13 (s, 1H), 8.06 (d, *J* = 7.9 Hz, 2H), 7.94 (s, 2H), 7.83-7.77 (m, 8H), 7.71 (d, *J* = 7.76 Hz, 2H), 7.62 (d, *J* = 7.76 Hz, 2H), 7.38 (d, *J* = 8.16 Hz, 2H), 7.25 (s, 2H), 6.95 (d, *J* = 8.15 Hz, 2H), 6.68-6.66 (m, 3H), 4.6 (s, 2H), 4.20 (m, 14H), 3.99 (t, *J* = 5.8 Hz, 2H), 3.89 (t, *J* = 7.75 Hz, 2H), 3.63 (s, 2H), 2.90-2.85 (m, 4H), 1.92 (m, 12H), 1.40-1.24 (m, 99H), 0.88 (m, 27H). ^{13}C NMR (100 MHz, $CDCl_3$), δ (ppm): 14.12, 16.50, 22.71, 25.97, 26.33, 27.07, 28.24, 28.98, 29.36, 29.42, 29.71,31.88, 53.45, 69.59, 69.73, 69.86, 70.92, 106.74, 107.44, 110.24, 118.74, 121.78, 123.23, 123.43, 123.47, 123.51, 124.05, 124.98, 125.95, 128.29, 131.34, 135.58, 138.01, 138.39, 139.53, 140.95, 142.98, 147.60, 148.95, 149.04, 149.24, 149.30, 149.36, 167.15. MALDI-MS (m/z): calcd. for $C_{131}H_{186}N_2O_{11}Pt$ [M^+] 2159.96, found 2159.65, 1568.14. Anal. Calcd for $C_{131}H_{186}N_2O_{11}Pt$: C, 72.84; H, 8.68; N, 1.30. Found: C, 72.20; H, 8.69; N, 1.36.

3. Results and discussion

3.1. Synthesis and characterized

The synthetic route of platinum complexes is depicted in **Scheme 1**. Starting from

the commercially available carbazole, intermediate **3** was obtained by Friedel-Crafts acylation and subsequent reduction reaction in 28% yield in two steps [46]. The following borylation of compound **3** with 2-isopropoxy-4,4,5,5-tetramethyl-1,3,2-dioxaborolane in the presence of *n*-BuLi gave intermediate **4** in 38% yield. Then, Suzuki coupling reaction between compound **4** and 2,5-dibromopyridine or 6-bromonicotinaldehyde yielded precursors **5** and **7**, respectively. Intermediate **5** reacted with compound **6** to afford cyclometalating ligand **LG-1** by Suzuki coupling reaction in the presence of $Pd(PPh_3)_4$. Compound **7** was reduced with $NaBH_4$ in toluene/ethanol solution at room temperature and then converted to intermediates **9** using 1,6-dibromohexane as the reactant. Cyclometalating ligand **LG-2** was obtained by etherification reaction between monohydroxypentaalkoxytriphenylene (**10**) and intermediate **9** using potassium carbonate in acetone solution. Target platinum complexes were finally synthesized according to the conditions reported by our group [40,41]. All the platinum complexes were confirmed by ^{1}H NMR, ^{13}C NMR, MALDI TOF-MS and elemental analysis (ESI†).

3.2. Thermal properties

The thermal stability of all platinum complexes was evaluated by TGA under a nitrogen atmosphere. All platinum complexes possess good thermal stability, with the decomposition temperature (T_d, 5% weight loss) above 270 ^{o}C, which is much better than the analogous platinum complexes TppyPtacac (162 ^{o}C) and TppyPtPhacac (191 ^{o}C) [43]. As seen from **Table 1**, the platinum complexes with dibenzoylmethane (DBM) moiety (**Pt6** and **Pt8**) are much more stable than the platinum complexes with

acetylacetone (acac) ligand (**Pt5** and **Pt7**). Additionally, the trend in thermal stability (**Pt5**<**Pt7**) clearly illustrates that the alkyl-chains length between triphenylene and platinum core has a positive impact on the thermal stability.

The mesomorphic behavior of these platinum complexes was investigated by DSC, POM and XRD. DSC scan was initially carried out to study the thermotropic property under nitrogen atmosphere. The DSC curves exhibit distinct patterns as a function of the molecular structure (ESI†). As for the platinum complexes with acac ligand (**Pt5** and **Pt7**), no clear endothermic peak and exothermic peak are found upon heating and cooling curves (**Table 1** and ESI†), which is similar to the previously reported triphenylene-based compounds [47-50]. In contrast, the platinum complexes with DBM ligand possess obviously phase transition peak owing to the more periphery alkyl chains. **Pt6** shows two endothermic peaks indicating multiple phase transitions upon heating process. However, the phase transition is not observed on cooling from DSC [45,49,51]. **Pt8** shows two endothermic peaks and one exothermic peak on cooling, respectively. Notably, the clearing point decreases with the increased length of the alkyl-chain between the triphenylene and the platinum core complex.

Based on the DSC results, POM results demonstrated that only **Pt6** showed fluidity and liquid crystal characters, with birefringence upon cooling. As shown in **Figure 1**, complex **Pt6** exhibits a branched leaf-like texture when cooling from the isotropic liquid, indicating a typical columnar phase [45,52]. Although **Pt5** presents an obviously birefringence phenomenon, it also seems to be some small crystals (**Figure 1**). In contrast, for complexes **Pt7** and **Pt8**, we did not detect any fluidity and

birefringence during heating and cooling (ESI†), in which both complexes possess crystalline state. Clearly, the length of alkyl chain between platinum complex skeleton and triphenylene unit has a crucial role on the mesomorphic behavior.

In order to further confirm the columnar phase of the platinum complexes, **Pt5** and **Pt6** were selected as representative examples to measure temperature-dependent X-ray diffraction (**Figure 2**). At 54 ^{o}C, as shown in **Figure 2**, the XRD pattern of **Pt6** shows one strong reflection at small angle range together with several small scatter peaks at low angle and high angle ranges, a feature of glassy (or partially crystalline) structure. When **Pt6** was heated to 185 ^{o}C, all the peaks disappear because of the formation of the isotropic phase. When the temperature is decreased to 116 ^{o}C from isotropic liquid, only a sharp reflection at 2θ of 3.2^{o} (27.6 Å) appears with a diffuse reflection at around 2θ of 18.4^{o} (4.8 Å), typical of the liquid crystalline state and assigned to the liquid-like order of the peripheral alkoxy chains [53,54]. Combined with DSC and POM observations, and compared to the XRD pattern at 54 ^{o}C, the disappearing of the diffraction peaks in the range of 5-15^{o} (2θ) and clearly changed XRD pattern at 116 ^{o}C indicates the formation of a mesophase. Due to the absence of more diffraction peaks in the high angle range, the exact mesophase structure could not be calculated. Nevertheless, according to literature reports about triphenylene-based compounds we assign the structure to a columnar phase [55-57]. However, for complex Pt5, the temperature-dependent XRD could not offer more evidences for the liquid crystalline state. Therefore, Pt5 was mainly tentative assigned to crystal structure.

3.3. Optical Properties

The absorption spectra of the complexes were measured in dichloromethane (CH_2Cl_2, 10^{-5} M) at room temperature (**Figure 3**), and the data are listed in **Table 2**. Each platinum complex shows three well-resolved absorption bands in the range of 250-500 nm. The intense absorption band from 250 to 310 nm with high molar absorptivities (ε) on the order of 10^5 M^{-1} cm^{-1} is assigned to the spin-allowed π-π* electron transitions of the cyclometalating ligand. Compared to **Pt5** and **Pt6**, the other platinum complexes show additional triphenylene absorption bands at about 280 nm, demonstrating the weak ground-state coupling between the platinum core and triphenylene unit due to the aliphatic spacer unit [58]. The moderately intense absorption band ranging from 310 to 370 nm (ε = 10^4 M^{-1} cm^{-1}) is attributed to intramolecular charge-transfer (ICT) and metal-to-ligand charge-transfer transitions (^{1}MLCT). The low-energy absorption band (>370 nm, 10^3-10^4 M^{-1} cm^{-1}) is ascribed to ^{3}MLCT transition according to previous report [58]. It is noted that the platinum complexes with DBM ligand (**Pt6** and **Pt8**) exhibit a stronger absorption in the range of 300-370 nm than the platinum with acac moiety (**Pt5** and **Pt7**). This result could be referred to electronic transitions involving the DBM moiety. Due to the expanded π-conjugation, **Pt5** and **Pt6** display a red-shifted absorption in low-energy region compared to other platinum complexes. Therefore the grafted aliphatic chain in cyclometalating ligand has a significant influence on their absorption property.

As shown in **Figure 4**, all platinum complexes display resolved vibrational emission spectra, generated from π-π* electron transitions. **Pt7** and **Pt8** show similar

emission spectra centered at 512 nm with a shoulder at about 547 nm. On the other hand, the PL spectra of **Pt5** and **Pt6** are red-shifted to 558 nm with respect to that of **Pt7** and **Pt8** caused by the expended π-conjugation. Compared to the analogous platinum complex TppyPtPhacac and TppyPtacac [43], **Pt5** and **Pt6** exhibit 8 nm red shift spectra due to the additional carbazole unit results in more effective intramolecular charge transfer transition, whereas **Pt7** and **Pt8** show hypochromatic shift spectra owing to the low conjugation caused by alkyl chains. The photoluminescence quantum yields (Φ) of these platinum complexes are in the range of 0.2-0.4 in degassed CH_2Cl_2. Interestingly, the emission peaks show little red shift in neat films relative to those in solution (ESI†). It is quite different from generally square planar platinum complex that **Pt5-Pt8** did not show distinct excimer emission in neat film, indicating the periphery alkyl and additional carbazole unit have an impact on suppressing the intermolecular aggregation.

3.4. Electrochemical Properties

The electrochemical properties of platinum complexes were evaluated by cyclic voltammetry in CH_2Cl_2 solution using ferrocene/ferrocenium (Fc/Fc^+) as an internal standard. All platinum complexes show the irreversible oxidation potentials between 0.39 V and 0.6 V (*vs* Fc/Fc^+, ESI†). Based on the oxidation potentials and optical band gap ($^{opt}E_g$), correspondingly, their highest occupied molecular orbital (HOMO) and lowest unoccupied molecular orbital (LUMO) levels are estimated via the formula of $E_{HOMO} = -(4.8 + E_{ox})$ eV and $E_{LUMO} = -(E_{HOMO} - {}^{opt}E_g)$ eV [59], respectively. As seen from **Table S1**, the ancillary ligand with DBM unit has a

stabilizing effect on HOMO and LUMO of the platinum complexes. All platinum complexes possess the energy band gaps from 2.63 to 2.82 eV (**Table S1**). **Pt5** and **Pt6** display relatively narrow energy band gaps compared to other platinum complexes, owing to the extended π-conjugation, which is also supported by absorption and emission properties.

3.5. Hole Mobilities

The hole mobilities of platinum complexes were also measured by the space charge limited current (SCLC) method with a device configuration of ITO/PEDOT:PSS (40 nm)/platinum complex (100 nm)/MoO_3 (10 nm)/Ag (100 nm). For the devices treated with thermal annealing (120^{o}C for 30 mins), these platinum complexes exhibit moderate hole mobilities in the range of 10^{-5}–10^{-6} cm^2 V^{-1} s^{-1} (**Table S2**, ESI†). Complex **Pt5** shows the best hole mobility up to 2.1×10^{-5} cm^2 V^{-1} s^{-1}. The results imply that the hole mobilities decreases with the increased aliphatic chains between the platinum core and triphenylene.

3.6. Polarized Devices

In order to systematically investigate the polarized EL of the platinum complexes, **Pt5** and **Pt6** were selected as the emitter. Poly(9,9'-dioctylfluorene) (PFO) was chosen as the host matrix because of its outstanding liquid crystalline and polarized emission [20,21]. Initially, the polarized OLEDs were fabricated with the configuration of ITO/PEDOT:PSS (30 nm)/PVK (30 nm)/PFO:platinum complex (94:6, 70 nm, rubbed)/B3YMPM (50 nm)/Ca (100 nm)/Al (100 nm). The polarized EL spectra recorded at 10 mA/cm^2 are depicted in **Figure 5** in terms of the emission intensity

parallel (H) and perpendicular to (V) the rubbing direction. In the case of **Pt5**-doped device, the polarized emission, with a dichroic ratio ($R = EL_H/EL_V$) of about 5, is only observed from blue emission of PFO (**Figure 5a**). For the **Pt6**-doped device, both blue emission from PFO and orange emission from platinum complex show polarized emission (**Figure 5b**). The *R* was evaluated to be 17.5 at 430 nm and 1.4 at 569 nm, respectively. This result indicates that complex **Pt5** has an inferior self-assemble property than **Pt6** in PFO film, which is also confirmed that **Pt5** could be crystal. Notably, the emission parallel to the rubbing direction is stronger than that perpendicular to the rubbing direction, implying the PFO and platinum complexes could be aligned with the rubbing [38].

To elucidate the effect of molecular order on polarized emission, a series of devices based on **Pt6** were fabricated with different procedures to prepare the aligned emissive layer (Experimental Section). The EL data of these devices are listed in **Table S3**. The aligned emissive layer in device **I** was processed without any special procedures. The emissive layer was annealed at 120 ^{o}C in device **II**. The emissive layer of device **III** was uniaxial rubbed for surface alignment, and then annealed at 120 ^{o}C, while the emissive layer in device **IV** was prepared via pressing on the surface, followed by annealing at 120 ^{o}C. Furthermore, to improve the quality of white light compared to the previous devices having a large blue component from PFO, the amount of Pt complex was increased to 20% in these devices in order to increase the red component.

Apparently, the EL emission varied with aligned emissive layer in different

polarized devices (**Figure 6** and ESI†). As depicted in **Figure 6**, Device **I** shows a broad EL emission from 400 nm to 750 nm. The blue emission in the range of 400-480 nm is attributed to host matrix PFO, while the low-energy emission (635 nm) are assigned to emission from electrically excited bimolecular species (electromers and electroplexes) as they are not observed in the PL emission in neat film [60]. The whole EL spectrum exhibits polarization dependence with *R* of 1.75 at 439 nm and 1.34 at 635 nm, respectively. This broad emission from device **I** has Commission Internationale de L'Eclairage (CIE) coordinates (0.43, 0.35), implying a nearly white emission. To the best of our knowledge, this is the first example of polarized white emission based on platinum complex.

When the emissive layer in devices **II-IV** was processed with thermal annealing, the deep red component of the emission spectra attributed to electromers/electroplexes significantly increases in intensity compared to device **I** (ESI†). Obviously, the annealed emitting layer has a significant effect on the EL emission, attributed to more ordered molecules and effective energy transfer between host matrix and guest. Device **II** shows the polarized EL with *R* of about 1 only at 670 nm, while device **III** displays the polarized emission at both blue emission (R = 5.5, 432 nm) and red emission (R = 1.1, 655 nm). However, the polarization dependence was not detected in device **IV**, which infers that it is difficult to align the emission film by pressing method. Compared to device **I**, devices **II-IV** show inferior polarized emissions, likely due to the poor alignment of the emissive layer. The CIE coordinates of devices **II-IV** have minor change from (0.51, 0.37) to (0.59, 0.35) in the reddish orange range.

Although these platinum metallomesogens show the charming polarized emission, the devices performances are still very low. Device **I** exhibits the best performance with a turn-on voltage of 6 V, a maximum luminance of 100 cd/m^2 and a current efficiency of 0.46 cd/A. Even though the efficiency achieved in these polarized devices is not fascinating compared to that of state-of-the-art phosphorescent OLEDs, it provides the strategy to achieve polarized white emission, which is necessary for the application of backlight in liquid crystal displays.

4. Conclusions

In summary, a series of novel platinum complexes were synthesized and characterized. Complex **Pt6** rather than **Pt5**, **Pt7** and **Pt8** can effectively form liquid crystalline, confirmed by DSC, POM and XRD. Compared to the reported TppyPtacac and TppyPtPhacac, this novel platinum complex showed better thermal stability and liquid crystal property. Additionally, the mesophase disappeared as the length of the alkyl-chain between platinum skeleton and triphenylene unit increased. The excimer emission can be effectively suppressed by periphery chains and additional carbazole units under opto-excitation. However, emission from electrically excited bimolecular species is observed in devices as a deep red, broad band. The exact nature of these species is not clear at this stage. As a result, the first example of polarized white electroluminescence rom a phosphorescent dopant was achieved with *R* of 1.4 in **Pt6**-based OLEDs. Importantly, the polarized EL was sharply dependent on the aligned emissive layer. Even though the performance of the polarized OLEDs is still frustrated, it is significant that current studies open up a new aspect of

phosphorescent metallomesogens application for the backlight of liquid crystal displays.

Acknowledgements

The authors sincerely thank Christopher Cabry and Prof. Duncan W. Bruce for XRD measurements. We are grateful for the financial support from the National Natural Science Foundation of China (21202139, 51473140 and 51273168), the Open Fund of

the State Key Laboratory of Luminescent Materials and Devices (South China University of Technology) (2015-skllmd-08), the European Union (MC-IIF-329199), and the Key Fund Project of Hunan Provincial Education Department (13A133).

.

Supporting Information

The Supporting Information is available free of charge on the Publications website. Detailed information on ^{1}H NMR, TOF-MS, TGA, DSC, POM, XRD, CV curves, hole mobility and polarized EL spectra.

References

[1] Kalinowskia J, Fattorib V, Cocchib M, Williamsc JAG. Light-Emitting Devices Based on Organometallic Platinum Complexes as Emitters. Coord Chem Rev 2011;255:2401-25.

[2] Williams JAG, Develay S, Rochester DL, Murphy L. Optimising the Luminescence of Platinum (II) Complexes and Their Application in Organic Light Emitting Devices (OLEDs). Coord Chem Rev 2008;252:2596-611.

[3] Williams JAG. The Coordination Chemistry of Dipyridylbenzene: N-Deficient Terpyridine or Panacea for Brightly Luminescent Metal Complexes? Chem Soc Rev 2009;38:1783-801.

[4] Brooks J, Babayan Y, Lamansky S, Djurovich PI, Tsyba I, Bau R, Thompson ME. Synthesis

and Characterization of Phosphorescent Cyclometalated Platinum Complexes. Inorg Chem 2002;41:3055-66.

[5] Chow PK, Cheng G, Tong GMS, To WP, Kwong WL, Low KH, Kwok CC, Ma C, Che C. Luminescent Pincer Platinum(II) Complexes with Emission Quantum Yields up to Almost Unity: Photophysics, Photoreductive C-C Bond Formation, and Materials Applications. Angew Chem Int Ed 2015;54:2084-9.

[6] Fleetham T, Li G, Wen L, Li J. Efficient "Pure" Blue OLEDs Employing Tetradentate Pt Complexes with a Narrow Spectral Bandwidth. Adv Mater 2014;26:7116-21.

[7] Fleetham T, Huang L, Li J. Tetradentate Platinum Complexes for Efficient and Stable Excimer-Based White OLEDs. Adv Funct Mater 2014;24:6066-73.

[8] Fukagawa H, Shimizu T, Hanashima H, Osada Y, Suzuki M, Fujikake H. Highly Efficient and Stable Red Phosphorescent Organic Light-Emitting Diodes Using Platinum Complexes. Adv Mater 2012;24:5099-103.

[9] Lin MY, Chen HH, Hsu KH, Huang YH, Chen YJ, Lin HY, Wu YK. White Organic Light-Emitting Diode With Linearly Polarized Emission. IEEE Photonic Tech L 2013;25:1321.

[10] Nguyen TD, Ehrenfreund E, Vardeny Z. The Spin-Polarized Organic Light Emitting Diode. Synth Met 2013;173:16-21.

[11] Pastoor S, Wijpking M. 3-D Displays: A Review of Current Technologies. Displays 1997;17:100-10.

[12] Liedtke M, Neill O, Wertmoller A, Kitney SP, Kelly M. White-Light OLEDs Using Liquid Crystal Polymer Networks. Chem Mater 2008;20:3579-86.

[13] Wang Y, Shi J, Chen J, Zhu W, Baranoff E. Recent Progress in Luminescent Liquid Crystal Materials: Design, Properties and Application for Linearly Polarised Emission. J Mater Chem C 2015;3:7993-8005.

[14] Dyreklev P, Berggren M, Inganäs O, Andersson MR, Wennerström O, Hjertberg T. Polarized Electroluminescence from An Oriented Substituted Polythiophene in A Light Emitting Diode. Adv Mater 1995;7:43-45.

[15] Geng Y, Culligan SW, Trajkovska A, Wallace JU, Chen SH. Monodisperse Oligofluorenes Forming Glassy-Nematic Films for Polarized Blue Emission. Chem Mater

2003;15:542-9.

[16] Culligan SW, Geng Y, Chen SH, Klubek K, Vaeth KM, Tang CW. Strongly Polarized and Efficient Blue Organic Light-Emitting Diodes Using Monodisperse Glassy Nematic Oligo(fluorene)s. Adv Mater 2003;15:1176-80.

[17] Klubek K, Vaeth KM, Tang CW. Monodisperse Glassy-Nematic Conjugated Oligomers with Chemically Tunable Polarized Light Emission. Chem Mater 2003;15:4352-60.

[18] Chen CA, Culligan SW, Geng Y, Chen SH, Klubek K, Vaeth K, Tang CW. Organic Polarized Light-Emitting Diodes via Förster Energy Transfer Using Monodisperse Conjugated Oligomer. Adv Mater 2004;16:783-8.

[19] Tokuhisa H, Era M, Tsutsui T. Polarized Electroluminescence from Smectic Mesophase. Appl Phys Lett 1998;72:2639-41.

[20] Grell M, Bradley DDC, Inbasekaran M, Woo EPA. Glass-Forming Conjugated Main-Chain Liquid Crystal Polymer for Polarized Electroluminescence Applications. Adv Mater 1997;9:798-802.

[21] Grell M, Knoll W, Lupo D, Meisel A, Miteva T, Neher D, Nothofer H, Scherf U, Yasuda A. Blue Polarized Electroluminescence from a Liquid Crystalline Polyfluorene. Adv Mater 1999;11:671-5.

[22] Tmiteva T, Meisel A, Grell M, Nothofer HG, Lupo D, Yasuda A, Knoll W, Kloppenburg L, Bunz UHF, Scherf U. Polarized Electroluminescence from Highly Aligned Liquid Crystalline Polymers. Synth Met 2000;111-112:173-6.

[23] Damm C, Israel G, Heqmann T, Tschierske C. Luminescence and Photoconductivity in Mononuclear *ortho*-Platinated Metallomesogens. J Mater Chem 2006;16:1808-16.

[24] Hegmann T, Kain J, Diele S, Schubert B, Bögel H, Tschierske C. Molecular Design at The Calamitic/Discotic Cross-Over Point. Mononuclear *ortho*-Metallated Mesogens Based on The Combination of Rod-Like Phenylpyrimidines and -Pyridines with Bent or Half-Disc-Shaped Diketonates. J Mater Chem 2003;13:991-1003.

[25] Kozhevnikov VN, Donnio B, Heinrich B, Williams JAG, Bruce DW. Green-Blue Light-Emitting Platinum (II) Complexes of Cyclometallated 4,6-Difluoro-1,3-dipyridylbenzenes Showing Mesophase Organisation. J Mater Chem C 2015;3:10177-87.

[26] Santoro A, Whitwood AC, Williams JAG, Kozhevnikov VN, Bruce DW. Synthesis, Mesomorphism, and Luminescent Properties of Calamitic 2-Phenylpyridines and Their Complexes with Platinum (II). Chem Mater 2009;21:3871-82.

[27] Spencer M, Santoro A, Freeman G, Diez A, Murry PR, Torroba J, Whitwood AC, Yellowlees LJ, Williams JAG, Bruce DW. Phosphorescent, Liquid-Crystalline Complexes of Platinum (II): Influence of The β-Diketonate Co-Ligand on Mesomorphism and Emission Properties. Dalton Tran 2012;41:14244-56.

[28] Kozhevnikov V, Donnio B, Bruce DW. Phosphorescent, Terdentate, Liquid-Crystalline Complexes of Platinum (II): Stimulus-Dependent Emission. Angew Chem Int Ed 2008;47:6286-9.

[29] Liao C, Chen H, Hsu H, Poloek A, Yeh H, Chi Y, Wang K, Lai C, Lee G, Shih C. Mesomorphism and Luminescence Properties of Platinum (II) Complexes with Tris(alkoxy)phenyl-Functionalized Pyridyl Pyrazolate Chelates. Chem Eur J 2011;17:546-56.

[30] Krikorian M, Liu S, Swager TM. Columnar Liquid Crystallinity and Mechanochromism in Cationic Platinum (II) Complexes. J Am Chem Soc 2014;136:2952-5.

[31] Jiang S, Luo K, Wang Y, Wang X, Jiang Y, Wei Y. Synthesis and Polarized Photoluminescence of Novel Phosphorescent Cyclometalated Platinum Dimer. Chin Chem Lett 2011;22:1005-8.

[32] Santoro A, Wegrzyn M, Whitwood AC, Donnio B, Bruce DW. Oxidation of Organoplatinum (II) by Coordinated Dimethylsulfoxide: Metal−Metal Bonded, Dinuclear, Liquid-Crystalline Complexes of Platinum (III). J Am Chem Soc 2010;132:10689-91.

[33] Llis M, Micutz M, Dumitrascu M, Pasuk L, Molard Y, Roisnel T, Cîrcu V. Enhancement of Smectic C Mesophase Stability by Using Branched Alkyl Chains in The Auxiliary Ligands of Luminescent P t(Ⅱ) and Pd (Ⅱ) complexes. Polyhedron 2014;69:31-9.

[34] Abe Y, Takagi Y, Nakamura M, Takeuchi T, Tanase T, Yokokawa M, Mukai M, Megumi T, Hachisuga A, Ohta K. Structural, Photophysical, and Mesomorphic Properties of Luminescent Platinum (II)-salen Schiff Base Complexes. Inorg Chim Acta 2012;392:254-60.

[35] Camerel F, Ziessel R, Donnio B, Bourgogne C, Guillon D, Schmutz M, Iacovita C, Bucher JP. Formation of Gels and Liquid Crystals Induced by Pt-Pt and π-π^* interactions in Luminescent σ-Alkynyl Platinum (Ⅱ) Terpyridine Complexes. Angew Chem Int Ed 2007;46:2659-62.

[36] Venkatesan K, Kouwer PHJ, Yaqi S, Müller P, Swager TM. Columnar Mesophases From Half-Discoid Platinum Cyclometalated Metallomesogens. J Mater Chem 2008;18:400-7.

[37] Díez A, Cowling SJ, Bruce DW. Polarised Phosphorescent Emission in An Organoplatinum (II)-Based Liquid-Crystalline Polymer. Chem Common 2012;48:10298-10300.

[38] Liu S, Lin M, Chen L, Hong Y, Tsai C, Wu C, Poloek A, Chi Y, Chen C, Chen S. Polarized Phosphorescent Organic Light-Emitting Devices Adopting Mesogenic Host-Guest Systems. Org Electron 2011;12:15-21.

[39] Tsai Y, Chen C, Chen L, Liu S, Wu C, Chi Y, Chen S, Hsu H, Lee J. Analyzing Nanostructures in Mesogenic Host-Guest Systems for Polarized Phosphorescence. Org Electron 2014;15:311-21.

[40] Wang Y, Liu Y, Luo J, Qi H, Li X, Ni M, Liu M, Shi D, Zhu W, Cao Y. Metallomesogens Based on Platinum (II) Complexes: Synthesis, Luminescence and Polarized Emission. Dalton Tran 2011;40:5046-51.

[41] Wang Y, Chen Q, Li M, Liu Y, Tan H, Yu J, Zhu M, Wu H, Zhu W, Cao Y. Highly Dichroic Metallomesogen of Dinuclear Platinum Complex: Synthesis and Liquid Crystal and Photophysical Properties. J Phys Chem C 2012;116:5908-14.

[42] Laschat S, Baro A, Steinke N, Giesselmann F, Hagele C, Scalia G, Judele R, Kapatsina E, Sauer S, Schreivogel A. Discotic Liquid Crystals: From Tailor-Made Synthesis to Plastic Electronics. Angew Chem Int Ed 2007;46:4832-87.

[43] Shi J, Wang Y, Xiao M, Zhong P, Liu Y, Tan H, Zhu M, Zhu W. Luminescent Metallomesogens Based on Platinum Complex Containing Triphenylene Unit. Tetrahedron 2015;71:463-9.

[44] Wang Y, Shi J, Zhu W, Liu Y, Tan H, Zhu M. The Chinese invention patent. CN104844661 A.

[45] . Wang Y, Zhang C, Wu H, Pu J. Synthesis and Mesomorphism of Triphenylene-Based Dimers With a Highly Ordered Columnar Plastic Phase. J Mater Chem C 2014;2:1667-74.

[46] Velasco D, Castellanos S, López M, López-Calahorra F, Brillas E, Juliá L. Red Organic Light-Emitting Radical Adducts of Carbazole and Tris(2,4,6-trichlorotriphenyl)methyl Radical That Exhibit High Thermal Stability and Electrochemical Amphotericity. J Org Chem 2007;72:7523-32

[47] Chen H, Zhao K, Wang L, Hu P, Wang B. Synthesis and Mesomorphism of Triphenylene Discotic Liquid Crystals Containing Fluorinated Chains. Soft Materials 2011;9:359-81.

[48] Tritto E, Chico R, Enguita ES, Folcia C, Ortega J, Coco S, Espinet P. Alignment of Palladium Complexes into Columnar Liquid Crystals Driven by Peripheral Triphenylene Substituents. Inorg Chem 2014;53:3449-55.

[49] Miao J, Zhu L. Columnar Liquid Crystalline Assembly of Doubly Discotic Supermolecules Based on Tetra-Triphenylene-Substituted Phthalocyanine. Soft Matter 2010;6:2072-79.

[50] Paraschiv I, Giesbers M, Lagen BV, Grozema FC, Abellon RD, Siebbeles LDA, Marcelis ATM, Zuilhof H, Sudhölter EJR. H-Bond-Stabilized Triphenylene-Based Columnar Discotic Liquid Crystals. Chem Mater 2006;18:968-974.

[51] Westphal E, Prehm M, Bechtold IH, Tschierske C, Gallardo H. Room Temperature Columnar Liquid Crystalline Phases of Luminescent Non-Symmetric Star-Shaped Molecules Containing Two 1,3,4-Oxadiazole Units. J Mater Chem C 2013;1:8011-22.

[52] Lin K, Kuo H, Sheu H, Lai C. Columnar Catenar Bisoxazoles and Bisthiazoles. Tetrahedron 2014;70:6457-66.

[53] Beltrán E, Garzoni M, Feringán B, Vancheri A, Barberá J, Serrano JL, Pavan G R, Giménez R, Sierra T. Self-Organization of Star-Shaped Columnar Liquid Crystals With a Coaxial Nanophase Segregation Revealed by a Combined Experimental and Simulation Approach. Chem Commun 2015;51:1811-4.

[54] Lehmann M, Maier P. Shape-Persistent, Sterically Crowded Star Mesogens: From Exceptional Columnar Dimer Stacks to Supermesogens. Angew Chem Int Ed 2015;54:9710-4.

[55] Paraschiv I, Tomkinson A, Giesbers M, Sudhölter EJ, Zuihof H, Marcelis ATM. Amide. Urea and Thiourea-Containing Triphenylene Derivatives: Influence of H-bonding on Mesomorphic Properties. Liquid Crystals 2007;34:1029-38.

[56] Wan W, Monobe H, Tanaka Y, Shimizu Y. Mesomorphic Properties of Copolyesters of

3,6-Linked Triphenylene-based Units and Polymethylene Spacers. Liquid Crystals 2003;30:571-8.

[57] Ba C, Shen Z, Gu H, Guo G, Xie P, Zhang R, Zhu C, Wan L, Li F, Huang CA. A Triphenylene-Containing Side Chain Liquid Crystalline Ladder-like Polysiloxane and Its Highly Ordered Superstructure. Liquid Crystals 2003;30:391-7.

[58] Denisov SA, Cudré Y, Verwilst P, Jonusauskas G, Suárez MM, Sánchez JFF, Baranoff E, McClenaghan ND. Direct Observation of Reversible Electronic Energy Transfer Involving an Iridium Center. Inorg Chem 2014;53:2677-82.

[59] Wang Y, Chen L, El-Shishtawy RM, Aziz SG, Müllen K. Synthesis and Optophysical Properties of Dimeric *aza*-BODIPY Dyes With a Push–Pull Benzodipyrrolidone Core. Chem Commun 2014;50:11540-2.

[60] Kalinowski J, Cocchi M, Marco PD, Stampor W, Giro G, Fattori V. Impact of High Electric Fields on The Charge Recombination Process in Organic Light-Emitting Diodes. J Phys D: Appl Phys 2000;33:2379-82.

Tables Captions

Table 1. Thermal properties of platinum complexes

Table 2. Photophysical parameter of platinum complexes

Table 1. Thermal properties of platinum complexes [a, b]

Complex	[c] T_g/°C	T_{onset}(°C)(⊿H(KJ/mol))	
		Phase →	Phase
Pt5	275	Cr (1.2) Iso	
Pt6	354	Cr 66 (10.3) Col 143 (3.6) Iso	
Pt7	306	–	
Pt8	364	Cr 88 (24.6) Cr′ 103 (22.3) Iso	

[a]Scan rate for all runs was 10 °C/min. [b]The phase transitions temperature was recorded at T_{onset} (the onset of second heating or first cooling). Phase nomenclature: Cr, Cr′ = crystal, Col = column mesophase, Iso = isotropic liquid. [c]The data were collected by TGA.

Table 2. Photophysical parameter of platinum complexes

Compounds	[a]UV-vis/nm (10^4 M^{-1} cm^{-1})	PL/nm		[c]Φ_{PL}
		[b]Solution	Film	
Pt5	267 (10.4), 294 (7.0), 341 (3.4), 410 (2.3), 433 (2.1)	561, 603	571, 618	0.35
Pt6	268 (8.4), 297 (11.0), 338 (8.1), 409 (4.0), 434 (2.8)	557, 598	577, 622	0.31

Pt7	270 (16.8), 280 (20.5), 297 (7.8), 348 (2.8), 391 (1.7)	511, 545	513, 551	0.19
Pt8	270 (14.8), 280 (18.0), 299 (7.6), 325 (6.0), 387 (3.6)	512, 547	508, 545	0.22

[a] the data were collected in CH_2Cl_2 solution; [b] the data were collected in degassed CH_2Cl_2 solution; [c] solutions of ppyPtacac (Φ_{PL} = 0.15) in 2-methyltetrahydrofuran were used as a reference.

Figures Captions

Chart 1 Molecular structures of **Pt5-Pt8**

Scheme 1 Synthetic route of platinum complexes

Figure 1 POM textures of **Pt5** (225 ^{o}C) and **Pt6** (111^{o}C) recorded on cooling.

Figure 2 XRD patterns of **Pt6** recorded at different temperatures.

Figure 3 UV-vis spectra of platinum complexes in CH_2Cl_2 solution at room temperature

Figure 4 PL spectra (excitation at 420 nm) of platinum complexes in CH_2Cl_2 at room temperature.

Figure 5 Polarized EL spectra measured at 10 mA/cm^2. (a: devices based on **Pt5**; b: devices based on **Pt6**. H: parallel, V: perpendicular)

Figure 6 Polarized EL spectra of devices I measured at 10 mA/cm^2. (H: parallel, V:

perpendicular)

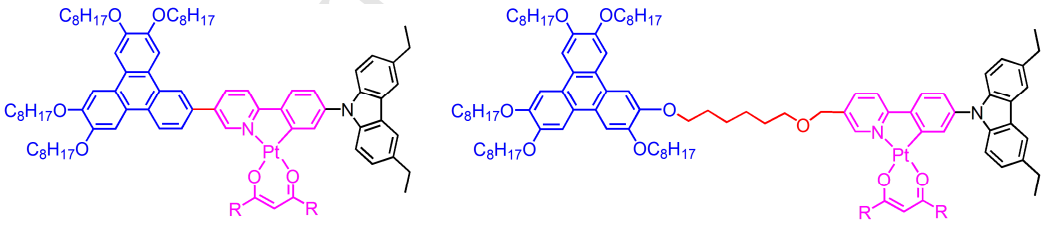

Chart 1 Molecular structures of **Pt5-Pt8**

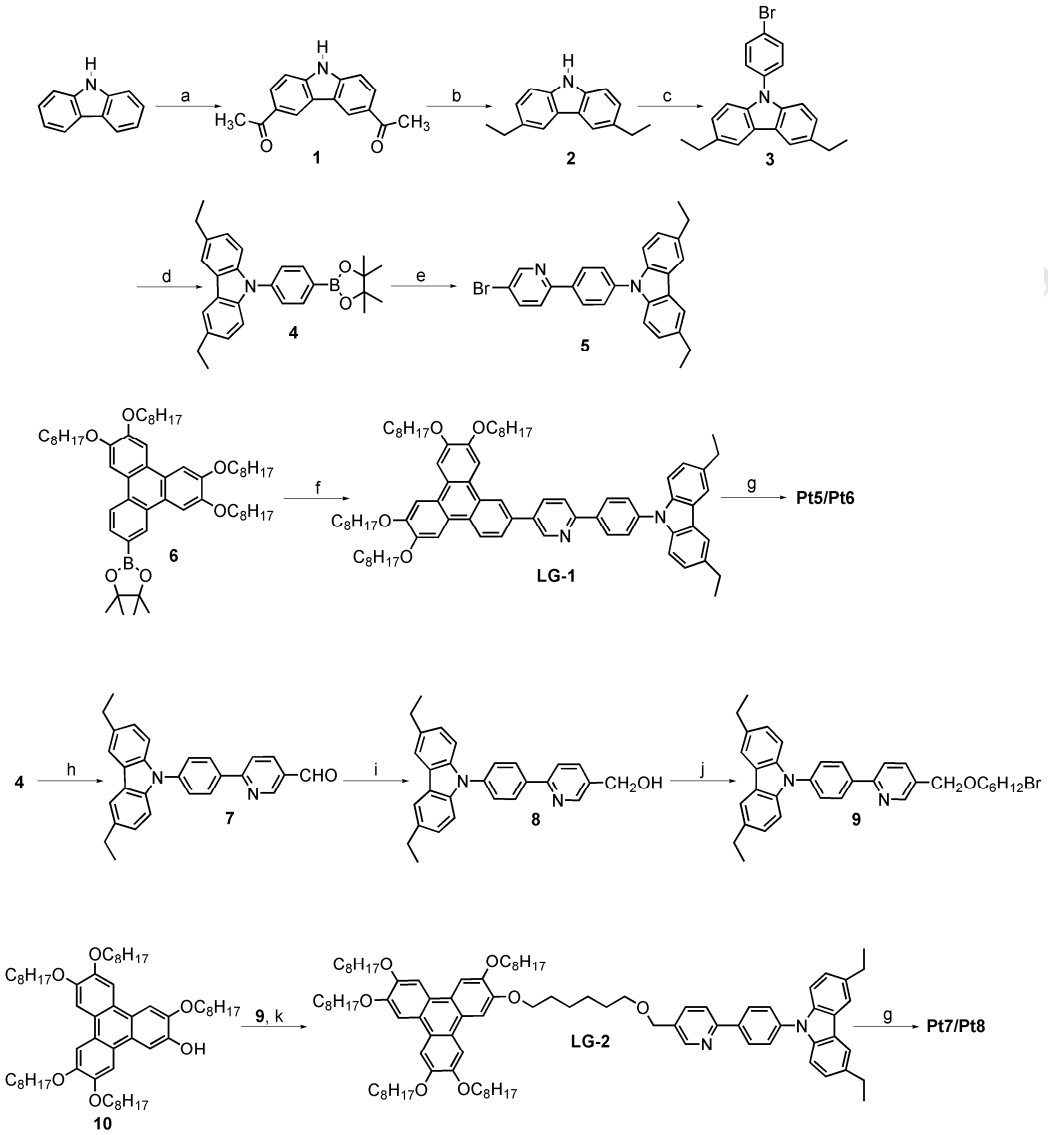

Reagents and conditions: (a) $AlCl_3$, CH_2Cl_2/0°C, CH_3COCl, overnight; (b) $AlCl_3$, THF, $LiAlH_4$, RT, 4 h; (c) 1-bromo-4-iodobenzene, K_2CO_3, phenanthroline, CuI, *o*-dimethylbenzene, reflux, 24 h; (d) 2-isopropoxy-4,4,5,5-tetramethyl-1,3,2-dioxaborolane, *n*-BuLi, THF, -78°C, overnight; (e) 2,5-dibromopyridine, Cs_2CO_3, $Pd(PPh_3)_4$, THF, reflux, 24 h; (f) $Pd(PPh_3)_4$, 2M Cs_2CO_3, toluene, 85°C, 24 h; (g) i: K_2PtCl_4, THF, H_2O, 80°C, 24 h; ii: Na_2CO_3, acac or DBM, 2-ethoxyethanol, 100°C, 24 h; (h) 2-Bromopyridine-5-carbaldehyde, $Pd(PPh_3)_4$, Cs_2CO_3(saturation), THF, reflux, 24 h; (i) $NaBH_4$, toluene/ethanol, RT, 6 h; (j) 1,6-dibromohexane, KI, NaOH (aq), acetone, reflux, 24 h; (k) 9, K_2CO_3, KI, acetone, reflux, 24 h.

Scheme 1 Synthetic route of platinum complexes

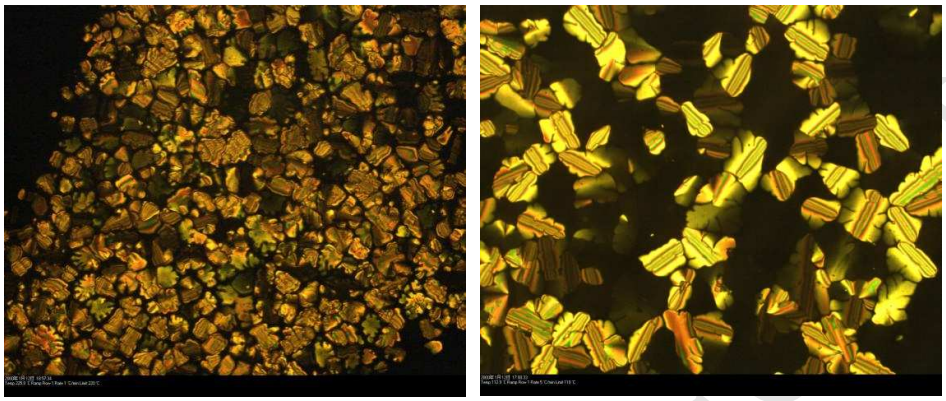

Figure 1 POM textures of **Pt5** (225 ^{o}C) and **Pt6** (111^{o}C) recorded on cooling.

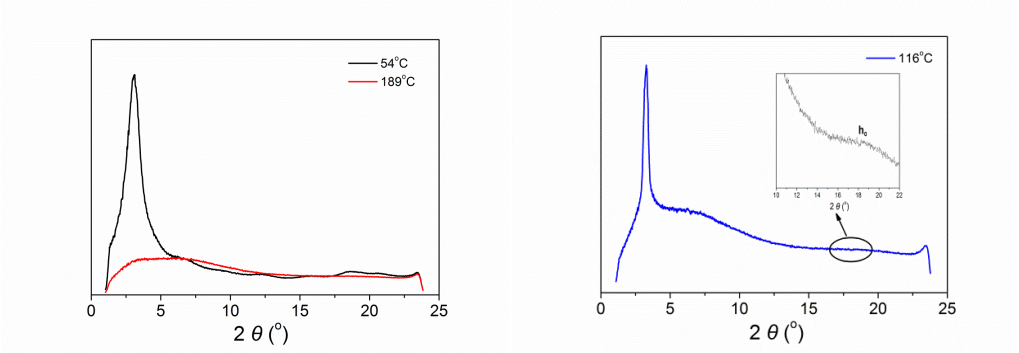

Figure 2 XRD patterns of **Pt6** recorded at different temperatures.

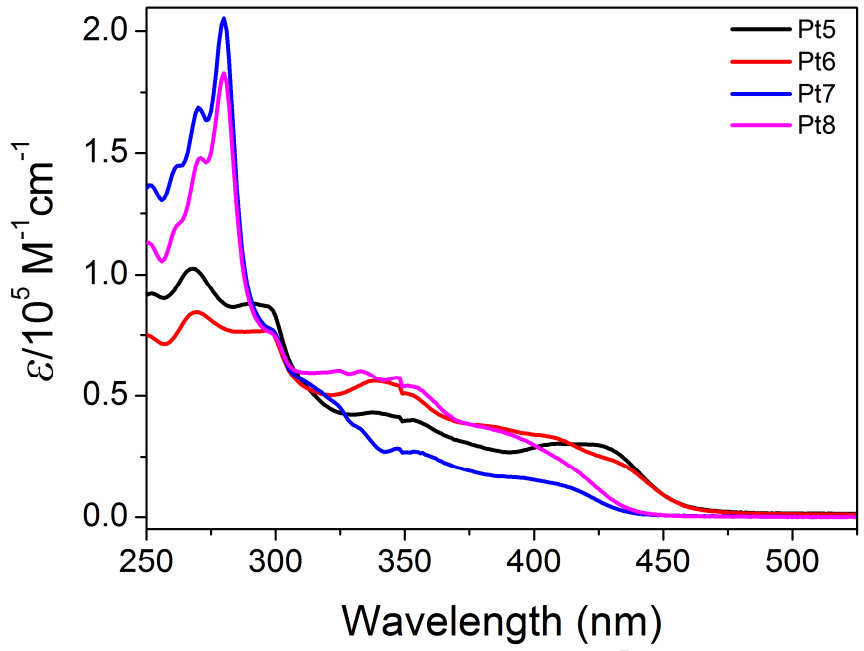

Figure 3 UV-vis spectra of platinum complexes in CH_2Cl_2 solution at room temperature

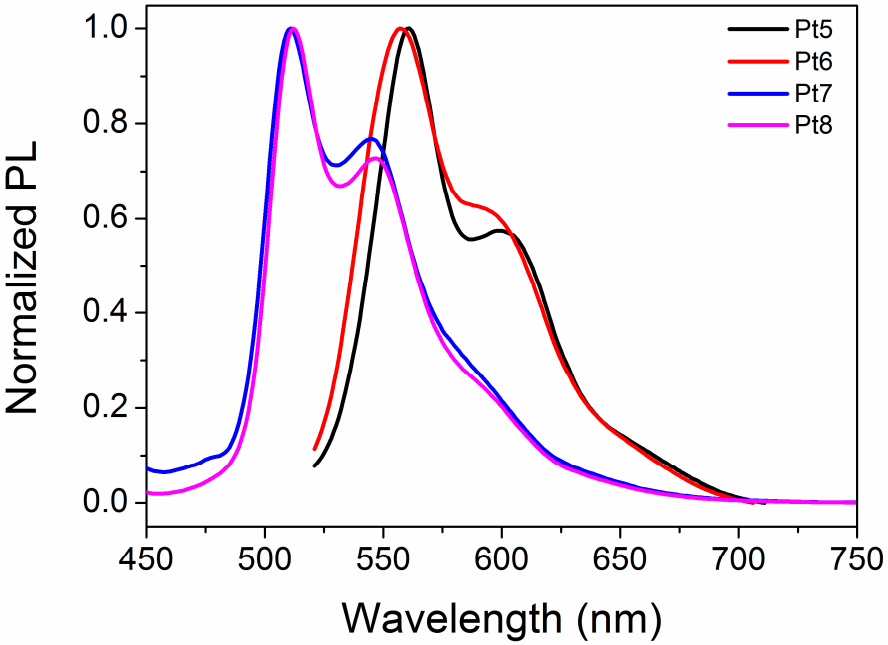

Figure 4 PL spectra (excitation at 420 nm) of platinum complexes in CH_2Cl_2 at room temperature.

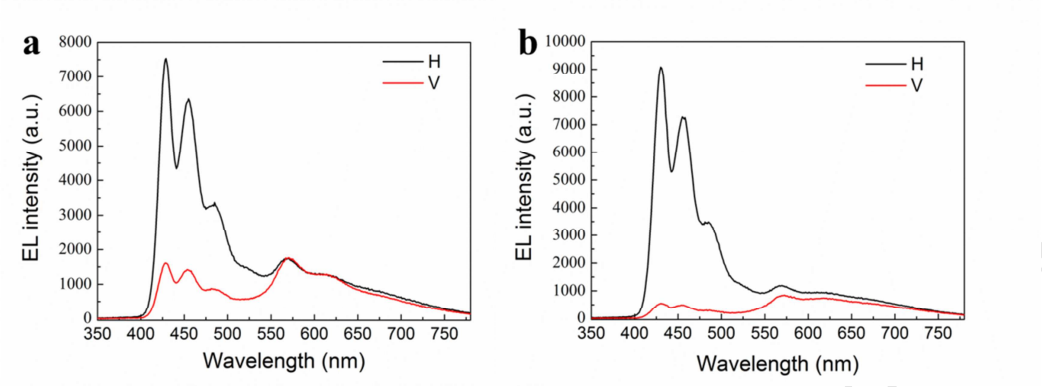

Figure 5 Polarized EL spectra measured at 10 mA/cm^2. (a: devices based on **Pt5**; b: devices based on **Pt6**. H: parallel, V: perpendicular)

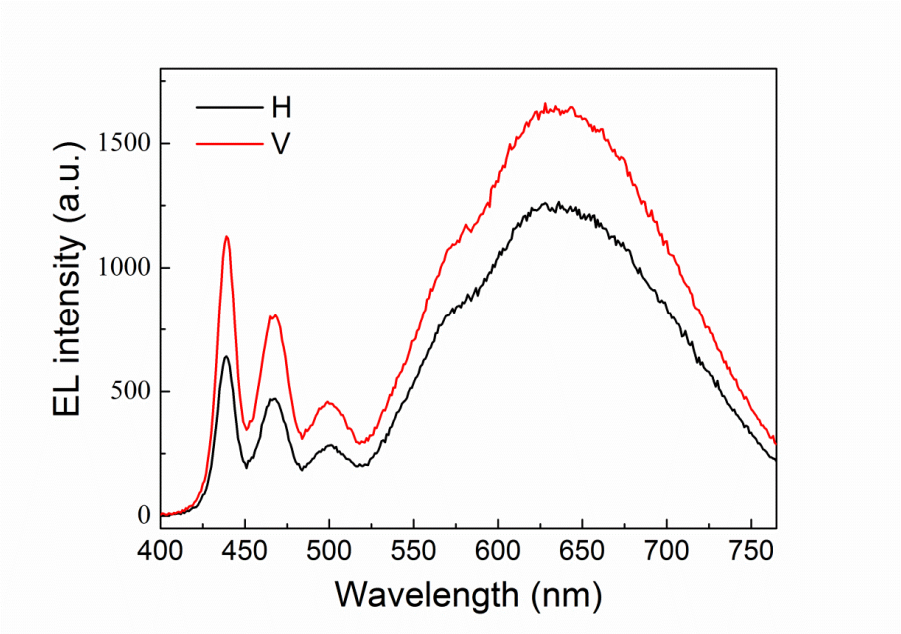

Figure 6 Polarized EL spectra of devices I measured at 10 mA/cm^2. (H: parallel, V: perpendicular)

Research Highlights

- A series of platinum complexes, Pt5-P8, containing triphenylene unit were prepared and characterized.
- Complex Pt6 exhibits a column phase evidenced by DSC, POM and XRD.
- All of platinum complexes show intense emission both in solution and solid state.
- Polarized white OLED with polarized ratio of 1.4 was achieved in **Pt6**-based device.